

# Flux Hamiltonians, Lie Algebras and Root Lattices With Minusculer Decorations

R. Shankar

*Sloane Laboratory of Physics, Yale University, New Haven, CN 06520  
Princeton Center for Theoretical Physics, Princeton University, Princeton, NJ 08544*

F. J. Burnell

*Department of Physics, Princeton University, Princeton, NJ 08544*

S. L. Sondhi

*Department of Physics, Princeton University, Princeton, NJ 08544  
Princeton Center for Theoretical Physics, Princeton University, Princeton, NJ 08544*

---

## Abstract

We study a family of Hamiltonians of fermions hopping on a set of lattices in the presence of a background gauge field. The lattices are constructed by decorating the root lattices of various Lie algebras with their minuscule representations. The Hamiltonians are, in momentum space, themselves elements of the Lie algebras in these same representations. We describe various interesting aspects of the spectra—which exhibit a family resemblance to the Dirac spectrum, and in many cases are able to relate them to known facts about the relevant Lie algebras. Interestingly, various realizable lattices such as the kagomé and pyrochlore can be given this Lie algebraic interpretation and the particular flux Hamiltonians arise as mean-field Hamiltonians for spin-1/2 Heisenberg models on these lattices.

---

## 1. Introduction and Outline

In this paper we study a family of Hamiltonians of fermions hopping around on various lattices in the presence of a background gauge field. These Hamiltonians are interesting to us, and we hope to the reader as well, in three distinct contexts: the search for flux phases in quantum magnets, the theory of Lie algebras, and their possessing interesting continuum limits with a family resemblance to the Dirac Hamiltonian. Let us now expand on these connections.

### 1.1. Flux phases

The first of these contexts is where we encountered them, which is the search for flux phases in quantum magnets. It was first noted by Baskaran, Zou, and Anderson [1,2] that a novel mean-field theory for  $SU(2)$  invariant spin-1/2 Hamiltonians could be constructed by re-representing spins as fermionic bilinears,  $\mathbf{S} = \bar{\psi}\boldsymbol{\sigma}\psi$ , and relaxing the constraint of a unit fermionic occupation of each site in favor of a global constraint of a half filled band. The mean-field treatment consists of replacing the starting Hamiltonian, quartic in the fermions, by one quadratic in them wherein the fermions hop on the lattice in the presence of a self-consistently calculated background (frozen) gauge field. Following this, Affleck and Marston [3] noted that

by extending the model to  $SU(N)$  spins this mean-field theory could be made exact at  $N = \infty$  whence it could serve as the starting point of a  $1/N$  expansion. Specifically, they showed that the Heisenberg model on the square lattice exhibited an enticing mean-field solution with a flux of  $\pi$  (a factor of  $e^{i\pi}$ ) per plaquette. Remarkably, they found that the solution to this hopping problem led to a Dirac fermion at zero energy. Since the system had particle-hole symmetry, and was at half-filling due to its insulating parentage mentioned above, the Dirac fermion was right at the Fermi energy and thus central to low energy physics. In particular, fluctuations around the saddle point were described by the Dirac fermion minimally coupled to the fluctuating gauge field. While it is tangential to our purposes in this paper, we note that the latter problem has been the focus of much progress in recent years [4]. Following these early developments, there has been much work examining various “flux phase” mean-field theories on various lattices which is too large a literature for us to review here.<sup>1</sup> Most interesting for our purposes was the generalization to time reversal (T) breaking phases made by Wen, Wilczek and Zee [9] which thus gave a mean-field meaning to the chiral flux phases proposed previously by Kalmeyer and Laughlin [10] on the basis of an inspired ansatz. These phases exhibit fluxes through closed loops which are different from the two T-invariant values 0 and  $\pi$ . There is one last aspect of this body of work that is also worth noting at the outset, namely that it does not take the actual energetics at  $N = \infty$ , and thus the relative stability of various mean-field solutions, too seriously. Strictly at  $N = \infty$  the kinds of solutions discussed above lose out to fully dimerized mean-field states of lower energy [11,12]. Their continuing interest has to do with the possibility that this relative ordering of energies is reversed as  $N$  is decreased. Indeed, the relative ordering between non-dimerized solutions could also change as  $N$  is decreased and hence one can (and people do), in good conscience, start out by studying various interesting mean-field solutions which at least exhibit local stability [5].

With the above recital we can now locate our Hamiltonians: they arise, with a few caveats and exceptions, as mean-field Hamiltonians for nearest-neighbor spin-1/2 Heisenberg Hamiltonians on the appropriate lattices. They also involve, in almost all cases, T-breaking.

## 1.2. Lie Algebras and Hamiltonians

There is, of course, a large set of such Hamiltonians and we next need to describe the restrictions that generate the family that we study. This brings us to the second context in which our Hamiltonians can be situated and which intrigues us most: the deep ties our Hamiltonians have to Lie algebras. These ties are twofold: ideas from Lie algebras are central to generating the very lattices the fermions move on and the Hamiltonians can be written as direct sums of pieces that are Lie algebra elements in specified representations. Consequently we find that properties of Lie algebras also control some striking features of the resulting spectra. Sometimes we fully understand these connections and sometimes we do not, though in all cases we will share what we know with the reader.

Let us first summarize how the unit cell and the underlying lattice have direct group theoretic significance. A discussion of the group theory used here can be found in [13,14].

Consider the unit cell. Recall that the generators of a (semi-simple) Lie algebras can be partitioned into a maximally commuting Cartan subalgebra  $H_i : [i = 1, \dots, r] = \mathbf{H}$  whose eigenvalues label the weights, and a set of ladder operators  $E_{\alpha}$  and their adjoints  $E_{\alpha}^{\dagger} = E_{-\alpha}$  that act on the states to raise (lower) the weights by  $\alpha$ . The vectors  $\alpha$  are called the roots. The states within any irreducible representation (multiplet) of a Lie algebra may therefore be visualized as a collection of points in a space of dimension  $r$ , called the rank. The coordinates of the points are the simultaneous eigenvalues of  $\mathbf{H}$ . The roots that help us move around these points are also vectors in the same space. For example, in the case of the rank-2 group  $SU(3)$ , (whose commuting quantum numbers are traditionally called isospin and hypercharge in the physics literature) the fundamental (quark) representation is an inverted triangle, the anti-quark is a triangle, and the eight-dimensional adjoint representation is a hexagon with two null weights at the center. The six nonzero roots correspond to the six corners of the hexagon.

<sup>1</sup> See, for example, [5], [6], [7] and references therein for more recent work in 2 d. A 3 d example and connections to the quantum Hall effect were addressed by [8].

The unit cells of the lattices we consider correspond to certain special representations called *minuscule representations*. Starting with any one state in a minuscule representation or multiplet, we can obtain all the others by acting with the Weyl group, the group of reflections about the hyper-planes normal to the roots. All weights of a minuscule representation are on the same footing and in particular all have the same length. Thus the quark and anti-quark are minuscule while the adjoint representation, with weights of both zero and non-zero length, is not.

This unit cell is now used to decorate a lattice, which is a subset of the root lattice  $L_R$ . Recall that roots, like weights, also live in  $r$  dimensions. So it is possible to choose  $r$  roots, called *simple roots*, as a basis. A basic result of group theory is that every root is an *integer* linear combination of the simple roots. There are of course a finite number of them in any algebra of rank  $r$ . The *root lattice*  $L_R$  is the infinite lattice formed with the same basis with but with *any* integer set of coefficients. For  $SU(3)$ , the six roots form a hexagon, while the root lattice is the infinite hexagonal lattice.

The lattice on which our fermions move is  $L_{2R}$ , the subset of  $L_R$  whose points have even integer coefficients, decorated by a basis corresponding to a minuscule representation.

When applied to the quark representation of  $SU(3)$ , this yields the kagomé lattice, as shown in Fig. 1(b). The inverted triangle (Fig. 1(a)) is the fundamental quark representation which forms the unit cell that decorates the root lattice  $L_{2R}$ , which is a hexagonal lattice with twice the lattice spacing as the root lattice  $L_R$ . The origin of coordinates is at the point named  $q$  in the figure. If you stare at the figure hard enough, you can also see it as a hexagonal lattice decorated by the conjugate representation, the anti-quark, whose weights are the negatives of the quark. The center of one such unit cell is labeled  $\bar{q}$  in the figure. The quark and anti-quark unit cells are corner sharing. These features are common to all our models and exist because the unit cell and the lattice are constructed from weights and roots in a particular way. A proof of this will be given in Section 2.1. Let us now turn to the construction of the Hamiltonians on the above set of lattices. Gauge fields will enter our models in the form of purely imaginary hopping amplitudes which can be  $\pm i$ . This restriction means that on any triangular face the flux can only be  $\pm\pi/2$ .<sup>2</sup> In other words the background gauge field is an Ising-like variable, and time reversal symmetry is broken. Also, we will require that the gauge fields exhibit the periodicity of the Bravais lattice  $L_{2R}$ — this has the gauge invariant content that there is no net flux passing through the lattice. It is worth noting here that generically in problems of this kind we must view symmetries as projective, i.e., the underlying group operations will have to be accompanied by additional gauge transformations to make the symmetry manifest [5], say the way Lorentz transformations have to be accompanied by gauge transformations in relativistic field theories to establish Lorentz covariance. The classification scheme relevant to our problem appears to be that of Color Groups, in which each face of the crystal is colored black or white, which we may read as  $\pm\pi/2$  of flux [15,16].

We are now in a position to specify the Hamiltonians of interest. Since the flux added to this lattice will be translationally invariant on  $L_{2R}$ , we may go to momentum space to solve for the dispersion relation. Evidently  $H(\mathbf{k})$  will be a matrix that acts on the states of the minuscule representation since they constitute the unit cell. With our choices of background gauge fields we then arrive at manifestly hermitian Hamiltonians of the form

$$H(\mathbf{k}) = \sum_{\alpha \in \Sigma^+} C_{\alpha}(\mathbf{k})(E_{\alpha} + E_{\alpha}^{\dagger}) \quad (1)$$

where the coefficients  $C_{\alpha}$  are real, satisfy

$$C_{\alpha}(-\mathbf{k}) = -C_{\alpha}(\mathbf{k}) \quad (2)$$

and  $\Sigma^+$  are the positive roots. The roots may be divided into positive ( $\Sigma_+$ ) and negative ( $\Sigma_-$ ) roots by drawing a plane through the origin which does not contain any roots. This choice is basis-dependent. For any choice of basis we may choose an ordering of the basis vectors so that the positive roots are those whose first nonzero component is positive.

Since the ladder operators move us around the multiplet, it is reasonable to consider  $H$  of the form (1). However we must bear in mind that this is not the most general possibility on this lattice. For example the model only allows hops between sites that differ by a *single* root while there are minuscule representations

<sup>2</sup> Evidently, the flux is the gauge invariant variable. Our choice of gauge fields is convenient for the purposes of this paper.

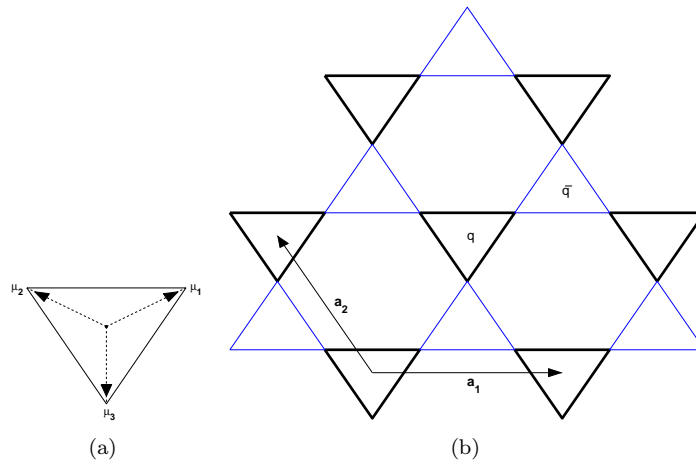


Fig. 1. The kagomé lattice and  $SU(3)$ : The unit cell (a) is the quark triplet, with weights  $\mu_1 \dots \mu_3$  as indicated. The kagomé lattice (b) is formed by decorating  $L_{2R}$  (the subset of the  $SU(3)$  root lattice with even integer coefficients) with this unit cell.  $L_{2R}$  is a hexagonal lattice with basis vectors  $\mathbf{a}_1$  and  $\mathbf{a}_2$  which are twice the simple roots of  $SU(3)$ . The origin of coordinates is marked  $q$ . The lattice may also be viewed as being decorated by anti-quark unit cells, one of which is centered at  $\bar{q}$

where the states differ by more than a single root. Other restrictions implied by this form of  $H$  will be discussed later.

Observe that we have obtained an unusual connection between the lattice and the hopping Hamiltonian: the former is obtained by decorating the root lattice of a Lie algebra with the weights of one of its representations, and the hopping Hamiltonian (in momentum space) is an element of the same Lie algebra in the same representation! It is worth emphasizing that this connection does not involve the symmetry group of the problem. For example, the Lie algebra  $SU(3)$  that shows up on the kagomé lattice does not generate the actual symmetries of the hopping problem or even correspond to any symmetries of the starting  $SU(2)$  Heisenberg model on that lattice.

One final point on the construction of our lattices and Hamiltonians: Although our lattice construction works in all dimensions, we shall limit ourselves to lattices in  $d = 2$  and  $d = 3$ , both because these are the dimensions we could encounter in the lab and because the rules for attaching flux break down in higher dimensions wherein areas cannot be oriented unambiguously. In this latter aspect the flux Hamiltonians that give rise to Dirac problems are special as they involve  $\pi$  flux, which does not carry an orientation, and thus their generalization to arbitrary dimensions is straightforward.

### 1.3. Dirac-like continuum limits

The discretized Laplace operator on lattices typically looks like a hopping problem with zero background flux. It is an interesting fact that when Kogut and Susskind [17] set out to discretize the Dirac operator on cubic lattices, they were naturally led to introduce a background flux of  $\pi$  per plaquette. Indeed, the Affleck-Marston work ended up “rediscovering” this earlier construction in the case of two spatial dimensions.

The flux Hamiltonians we consider evidently have a family resemblance to the  $\pi$  flux Hamiltonians which they generalize. It is also the case that their low energy limits exhibit a family resemblance to the Dirac theory which is the third context in which they appear to be interesting.

As a first step in explaining what we mean let us observe that zero energy plays a special role in our entire set of Hamiltonians. Normally, this comes about via a particle-hole symmetry, where at every momentum  $\mathbf{k}$  states at energy  $E$  are accompanied by states at  $-E$ . In our problems, the choice of background flux ensures that  $H(-\mathbf{k}) = -H(\mathbf{k})$ . Consequently for every level that is negative and hence occupied at  $\mathbf{k}$ , there is one at  $-\mathbf{k}$  that is empty and unoccupied so that the combination of the two bands is particle-hole symmetric and  $E = 0$  is again special. We should observe that this is very useful in the original context of the mean-

field theory of various Heisenberg models for this ensures that the half-filled band exhibits a Fermi energy,  $E_F = 0$ .

In the  $\pi$  flux phase, the structure about  $E = 0$  is that of the Dirac theory. In our examples we find generalizations that we term Dirac-like or pseudo-Dirac. By Dirac-like, we mean a generalization in three respects. First, although the spectrum is linear in momentum for small momentum, it possesses only discrete and not full rotational invariance. Second, the square of the Hamiltonian  $H$  is not proportional to the unit matrix, though a higher degree polynomial is. While a result of this sort is inevitable for any finite size matrix, the fact that the polynomial often contains just even powers leads to a result that is sufficiently reminiscent of the Dirac case. The third generalization we encounter is that in addition to isolated Dirac (or Dirac-like) points, we often find entire lines and even planes of zero energy.

The zeros are interesting in and of themselves in the Lie algebraic setting: in some cases, the lines of zeros are along the direction of the weights while in other cases the planes of zeros are simply related to the roots and so on. In some cases we can understand the locus of zeros without explicit computation by appealing to ideas from group theory, while in many cases we could neither anticipate nor explain the zeros.

There is, inevitably, a matrix structure that goes with the low energy Dirac-like theory and generalizes the gamma matrices but it does not appear to be immediately interesting in and of itself although we will exhibit it in one especially interesting case.

#### 1.4. *What follows*

In Section 2 we explain the construction of the lattice in detail, and describe the examples we will study in the remainder of the paper. We discuss the hopping problem for the  $d = 2$  lattices in Section 3, studying several possible background fluxes. In Section 4 we carry out the same analysis for lattices in  $d = 3$ . Here the reader can find in some detail a discussion of the pyrochlore lattice, which we understand the best in terms of group theory and which also displays interesting mathematical structures. In Section 5 we comment on the utility of our Hamiltonians as mean-field solutions of the Heisenberg model on our various lattices and on two extensions of our analysis. Section 6 contains concluding remarks and discusses open problems.

## 2. Lattice construction

Recall our recipe for generating the lattices:

- Generate  $L_{2R}$ , the even sector of the root lattice, that is to say, even integer combinations of the simple roots.
- Decorate each lattice point with a minuscule representation.

As noted in the Introduction, although our lattice construction works in all dimensions, we shall limit ourselves to lattices in  $d = 2$  and  $d = 3$ , due to their physical relevance and more absolutely because the rules for attaching flux break down in higher dimensions wherein areas cannot be oriented unambiguously. Hence we study rank 2 and 3 groups only. Here is the list of candidates.

- $d = 2$ :  $SU(3)$  and  $SO(5)=Sp(4)$ . The exceptional group  $G_2$  does not have minuscule representations. The group  $SO(4)$  factors into two independent  $SU(2)$  factors and will only be discussed very briefly.
- $d = 3$ :  $SU(4)=SO(6)$ ,  $SO(7)$ , and  $Sp(6)$ . There are no exceptional groups of rank 3.

The minuscule representations in each case will be listed as we go along.

### 2.1. *Properties of our lattices.*

The lattices we manufacture by the rules listed above have some interesting features that will be established in this section. Before we do so in general, let us pause to examine a simple example, the rank-2 group  $SU(3)$ . This exercise will help us better motivate and understand the general case.

The only minuscule representations are the quark and antiquark. Let us begin with the quark representation.

The weights, numbered 1, 2, 3 in Fig. 1(a), are

$$\boldsymbol{\mu}_1 = \frac{1}{2}(1, \frac{1}{\sqrt{3}}), \quad \boldsymbol{\mu}_2 = \frac{1}{2}(-1, \frac{1}{\sqrt{3}}), \quad \boldsymbol{\mu}_3 = (0, -\frac{1}{\sqrt{3}}) \quad (3)$$

and point to the vertices of an equilateral triangle.

One significant feature of these weights that we will invoke is that

$$\boldsymbol{\mu}_i \cdot \boldsymbol{\mu}_j = \begin{cases} a & i = j \\ b & i \neq j \end{cases} \quad (4)$$

where  $a = 1/3$  and  $b = -1/6$ . In other words, there are just two possible values for  $\boldsymbol{\mu}_i \cdot \boldsymbol{\mu}_j$ , between a weight and itself ( $a$ ) and between a weight and any other ( $b$ ).

The nice thing about  $SU(3)$  is that in the quark representation, the weights form a simplex where every corner is equidistant from every other, the difference between any two corners (any side of the simplex) is a root, and these are the only roots. Note that this implies six roots for  $SU(3)$ , since each edge of the triangle can be traversed in two directions. So the root system of  $SU(3)$  is

$$\Sigma(SU(3)) = \boldsymbol{\mu}_i - \boldsymbol{\mu}_j \equiv \boldsymbol{\alpha}_{ij} \quad [i \neq j : 1, 2 \text{ or } 3] \quad (5)$$

We may choose the simple roots to be  $\boldsymbol{\alpha}_{12}$  and  $\boldsymbol{\alpha}_{23}$  and in terms of them the lattice  $L_{2R}$  is defined as the set of points

$$\begin{aligned} 2\mathbf{R} &= 2m\boldsymbol{\alpha}_{12} + 2n\boldsymbol{\alpha}_{23} \\ &\equiv m\mathbf{a}_1 + n\mathbf{a}_2 \end{aligned} \quad (6)$$

We can now put the expanded root lattice together with the minuscule representation: in Fig. 1(b) we have placed one triangle at the origin (labeled  $q$ ) and made copies at every lattice point in  $L_{2R}$ . As the reader can see, we end up with the kagomé lattice.

Let us note that the two features, Eqs. (4,5), generalize in the obvious manner for all  $SU(N)$ , where the weights now point to the vertices of an  $N$ -simplex.

Now we turn to some general features of our lattices valid for all the groups we will study, not dependent on the special features of  $SU(N)$  alluded to above. To see what they might be, look at Fig. 1(b), and observe the following features:

- (i) The lattice can also be viewed as  $L_{2R}$  decorated by the conjugate (anti-quark) representation with reversed weights. The original representation and the conjugate share corners, and every site is shared in this manner.
- (ii) If the particle can hop to any point labeled  $i$  from a point labeled  $j$  in the same unit cell by moving a displacement  $\mathbf{d}_{ij}$ , it can keep moving an extra  $\mathbf{d}_{ij}$  to reach a point labeled  $j$  in the adjacent unit cell. In other words the edges of the unit cell and the conjugate unit cell that meet at a shared corner are continuations of each other with no change in direction.

We will now furnish the proofs of these results in the general case.

**Theorem I:** The original lattice  $2\mathbf{R} + \boldsymbol{\mu}_i$  can be rewritten as  $2\mathbf{R} + 2\boldsymbol{\mu}_1 - \boldsymbol{\mu}_i$ . In other words, if at a new origin displaced from the old one by  $2\boldsymbol{\mu}_1$ , we place the conjugate representation and make copies of it using any element of  $L_{2R}$ , we get the old lattice. The result is just as valid if we use any other weight  $2\boldsymbol{\mu}_j$  in place of  $2\boldsymbol{\mu}_1$ .

**Proof:**

$$2\mathbf{R} + 2\boldsymbol{\mu}_1 - \boldsymbol{\mu}_i = 2\mathbf{R} + 2\boldsymbol{\mu}_1 - 2\boldsymbol{\mu}_i + \boldsymbol{\mu}_i = 2\mathbf{R}' + \boldsymbol{\mu}_i \quad (7)$$

where we have used the fact that  $2\boldsymbol{\mu}_1 - 2\boldsymbol{\mu}_i$ , being an even integer multiple of weight differences, is then an even integer multiple of roots, which in turn is a translation within  $L_{2R}$ .

Note that the choice of origin at  $2\boldsymbol{\mu}_1$  is arbitrary: the choice  $2\boldsymbol{\mu}_2$  differs by  $2\boldsymbol{\mu}_2 - 2\boldsymbol{\mu}_1$ , an even integer multiple of roots, and hence a translation within  $L_{2R}$ . ■

**Theorem II** If the particle can hop to any point labeled  $i$  from a point labeled  $j$  in the same unit cell by moving a distance  $\mathbf{d}_{ij}$ , it can keep moving an extra  $\mathbf{d}_{ij}$  to reach a point labeled  $j$  in the adjacent unit cell.

**Proof:** Since  $\mathbf{d}_{ij}$  is a difference of weights it is some integer combination of simple roots. Moving an extra distance  $\mathbf{d}_{ij}$ , corresponds to a total displacement by an even integer combination of simple roots, which is a symmetry of  $L_{2R}$ . It follows that if we start at a point labeled  $j$  we must end up a point also labeled  $j$ . ■

## 2.2. Lattices in $d = 2$

We have already discussed  $SU(3)$  in the last section. Now we will deal with  $SO(5)$  and  $Sp(4)$ . These two Lie algebras are mathematically equivalent up to cosmetic differences which will be displayed.

### 2.2.1. $SO(5)$

We begin with the more familiar group  $SO(5)$  which preserves the norm

$$x^2 = \sum_{i=1}^5 x_i^2 \quad (8)$$

and has a defining representation of  $5 \times 5$  orthogonal matrices.

We choose as Cartan generators  $H_1 = L_{12}$  and  $H_2 = L_{34}$  which generate rotations in the 12 and 34 planes. In terms of the coordinates

$$x_I^\pm = \frac{x_1 \pm ix_2}{\sqrt{2}} \quad x_{II}^\pm = \frac{x_3 \pm ix_4}{\sqrt{2}} \quad x_0 = x_5 \quad (9)$$

we may write the invariant in this spherical basis as

$$x^2 = x_0^2 + 2 \sum_{a=I}^{II} x^{-a} x_a . \quad (10)$$

The vector  $x$  itself serves as a 5-dimensional representation. The components  $x_I^\pm$  and  $x_{II}^\pm$  are eigenstates of  $H_1, H_2$  with eigenvalues  $\mathbf{H} = (\pm 1, 0)$  and  $(0, \pm 1)$  while  $x_0 = x_5$  does not respond to either rotation and has eigenvalues  $(0, 0)$ . The vector representation is not minuscule since the weights are of unequal length.

The only minuscule representation is the 4-component spinor, with weights

$$\boldsymbol{\mu} = \left( \pm \frac{1}{2}, \pm \frac{1}{2} \right) . \quad (11)$$

These form a square as in Fig. 2(a).

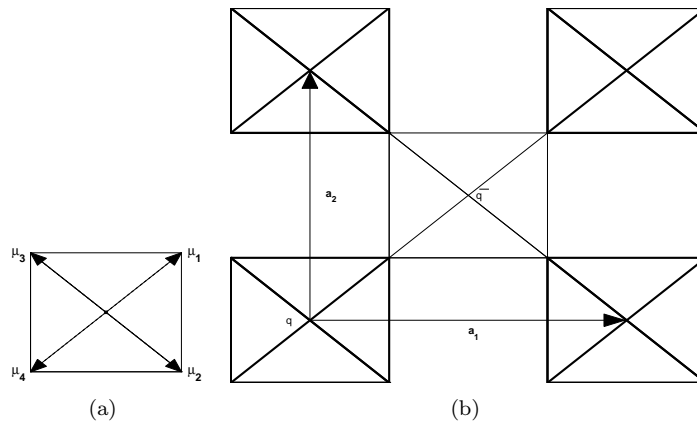


Fig. 2. Planar pyrochlore and  $SO(5)$ : The unit cell (a) of the spinor representation is the square of edge unity. The resulting square lattice, with hoppings along all roots, is shown in (b). The lattice vectors  $\mathbf{a}_1, \mathbf{a}_2$  are a basis for the subset of the  $SO(5)$  root lattice with even integer coefficients.

The eight roots for  $SO(5)$  are given by

$$\Sigma(SO(5)) = \pm \mathbf{e}_i; \pm \mathbf{e}_i \pm \mathbf{e}_j \quad i \neq j = 1, 2 \quad (12)$$

where  $\mathbf{e}_i$  is a unit vector in direction  $i$ . The short roots connect states along the coordinate axes while the long ones go diagonally.

The same spinor also forms a representation of  $SO(4)$ . However  $SO(4)$  has only the four long roots and one can see that the weights  $\pm(\frac{1}{2}, \frac{1}{2})$  do not talk to the pair  $\pm(\frac{1}{2}, -\frac{1}{2})$ , which means the representation is reducible. We do not discuss it here.

The simple roots are  $\mathbf{e}_1 - \mathbf{e}_2$  and  $\mathbf{e}_2$ ; our root lattice is  $2\mathbf{R} = 2m(\mathbf{e}_1 - \mathbf{e}_2) + 2n\mathbf{e}_2 = 2m'\mathbf{e}_1 + 2n'\mathbf{e}_2$ , a square lattice of sides 2. A site on the decorated lattice is  $2\mathbf{R} + (\pm\frac{1}{2}, \pm\frac{1}{2})$ .

Since the spinor is self-conjugate, the original squares share corners with identical squares, and the resulting lattice is the square lattice. When links along the long roots are included as in Fig. 2(b), the structure is known variously as the square lattice with crossings (SLWC), checkerboard lattice, or planar pyrochlore. Note also that if you can hop from site  $j$  to site  $i$  on one unit cell, you can hop once more by the same amount to hit site  $j$  in the next unit cell.

### 2.2.2. $Sp(4)$

The weights of the 4-dimensional minuscule representation of  $Sp(4)$  are

$$\boldsymbol{\mu} = (\pm 1, 0), (0, \pm 1). \quad (13)$$

Since the group is the collection of  $4 \times 4$  symplectic matrices, this is also called the defining representation. (The same terminology applies, say to the 6-dimensional vector representation of  $SO(6)$ , which is the group of  $6 \times 6$  orthogonal matrices.)

The roots of  $Sp(4)$  are

$$\Sigma(Sp(4)) = \pm\mathbf{e}_i \pm \mathbf{e}_j \text{ and } \pm 2\mathbf{e}_i \quad i \neq j : 1, 2 \quad (14)$$

Now the long roots connect points parallel to the axes and short roots in diagonal directions, as shown in Fig. 3(a). Note that this is just the rotated and rescaled version of  $SO(5)$ .

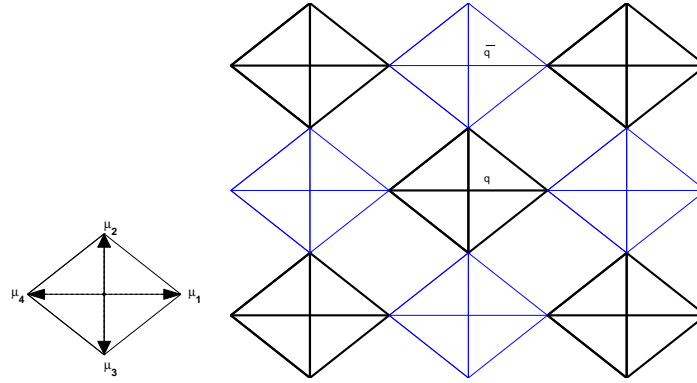


Fig. 3. Planar pyrochlore and  $Sp(4)$ : The unit cell (a) for the defining representation of  $Sp(4)$  is the square rotated by 45 degrees. The entire lattice (b) is the rotated version of the  $SO(5)$  spinor.

This concludes the enumeration of lattices in  $d = 2$ .

### 2.3. Lattices in $d = 3$

With the warm up from  $d = 2$  we can proceed rapidly through  $d = 3$  where the candidates are  $SU(4)=SO(6)$ ,  $Sp(6)$ , and  $SO(7)$ .

#### 2.3.1. $Sp(6)$

The only minuscule representation for  $Sp(6)$  is the defining 6-dimensional one. The weights are

$$\boldsymbol{\mu} = (\pm 1, 0, 0), (0, \pm 1, 0), (0, 0, \pm 1) \quad (15)$$



which form an octahedron which is self-conjugate. The decorated lattice is most readily visualized as corner sharing octahedra, which we will refer to as the octachlore lattice, depicted in Fig. 4. The roots are

$$\Sigma(Sp(6)) = \pm \mathbf{e}_i \pm \mathbf{e}_j \quad \text{and} \quad \pm 2\mathbf{e}_i \quad i \neq j : 1, 2 \text{ or } 3 \quad (16)$$

The short roots allow you to hop along the edges of the octahedron while the long roots take you straight across the unit cell to the antipodal point. This is just the  $d = 3$  version of  $Sp(4)$ .

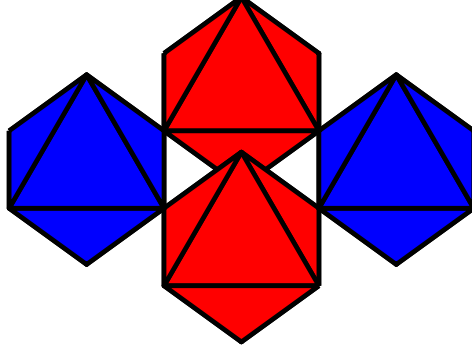


Fig. 4. The octachlore lattice of  $SP(6)$ : blue octagons are copies of the defining representation of  $Sp(6)$ ; red octagons are in the conjugate representation. Note that we have not drawn the bonds along the long roots.

### 2.3.2. $SO(7)$

Next we turn to  $SO(7)$ . Only the spinor is minuscule. It has self-conjugate weights

$$\boldsymbol{\mu} = (\pm \frac{1}{2}, \pm \frac{1}{2}, \pm \frac{1}{2}) \quad (17)$$

which lie at the corners of a unit cube. The roots

$$\Sigma(SO(7)) = \pm \mathbf{e}_i \pm \mathbf{e}_j \quad \text{and} \quad \pm \mathbf{e}_i \quad i \neq j : 1, 2 \text{ or } 3 \quad (18)$$

allow hops along edges, and diagonally across faces, but not along the body-diagonal. The root lattice  $L_{2R}$  is cubic with edges of size 2. The decorated lattice is made of corner sharing unit cubes, with face diagonal hopping on every second cube as one proceeds along any of the three cubic axes (Fig. 5). This is one possible 3 dimensional variant of the checkerboard lattice discussed in Sections 2.2.2 and 2.2.1; we shall refer to it as the 3 dimensional checkerboard lattice. The other, which we will discuss in the next section, is the pyrochlore.

In higher dimensions the  $SO(2N + 1)$  spinor leads to the N-dimensional checkerboard lattice: an N dimensional cubic lattice with links on all face diagonals.

### 2.3.3. $SO(6)$

We obtain  $SO(6)$  from  $SO(7)$  if we drop the short roots  $\pm \mathbf{e}_i$ :

$$\Sigma(SO(6)) = \pm \mathbf{e}_i \pm \mathbf{e}_j \quad i \neq j : 1, 2 \text{ or } 3. \quad (19)$$

Consider the spinor representation of  $SO(7)$ . Without the short roots  $\pm \mathbf{e}_i$ , we can only flip the signs of the components of each weight two at a time. This means the 8-dimensional spinor of  $SO(7)$  breaks down into two irreducible representations with four weights each. The first has an even number of negative weights

$$\boldsymbol{\mu}_1 = (\frac{1}{2}, \frac{1}{2}, \frac{1}{2}), \quad \boldsymbol{\mu}_2 = (-\frac{1}{2}, -\frac{1}{2}, \frac{1}{2}), \quad \boldsymbol{\mu}_3 = (\frac{1}{2}, -\frac{1}{2}, -\frac{1}{2}), \quad \boldsymbol{\mu}_4 = (-\frac{1}{2}, \frac{1}{2}, -\frac{1}{2}) \quad (20)$$

and the other has these weights reversed and hence an odd number of negative weights. This is general: the irreducible spinor of  $SO(2N + 1)$  becomes two irreducible representations of  $SO(2N)$ , called left and right handed spinors.

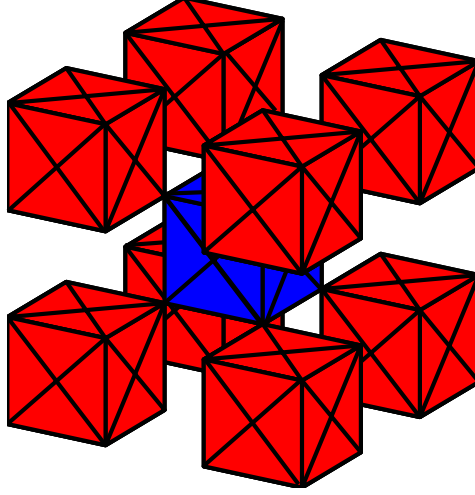


Fig. 5. The 3-d checkerboard  $SO(7)$  spinor lattice: blue and red cubes show the spinor representation and its conjugate (identical in this case).

If you join the 4 points in either spinor multiplet, you will see the tetrahedra that form the weights of the  $SU(4)$  quark and antiquark representations. In other words the right and left handed spinors of  $SO(6)$  are the quark and anti-quark of  $SU(4)$ . (This is why we will not study  $SU(4)$  separately.) The tetrahedra form the familiar pyrochlore lattice shown in Fig. 6.

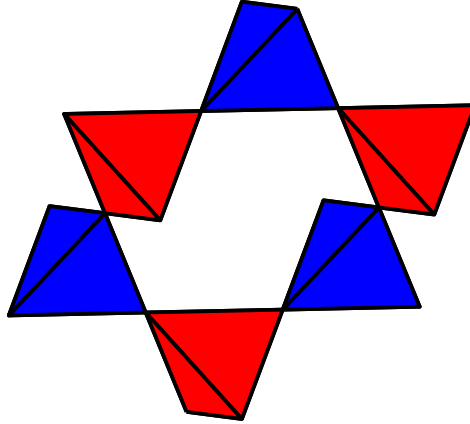


Fig. 6. The pyrochlore  $SO(6)$  spinor lattice: Blue tetrahedra are in the fundamental representation of  $SU(4)$ , or the right-handed spinor representation of  $SO(6)$ ; red tetrahedra are in the conjugate representation.

The extensions of this construction to higher dimensions yield corner sharing simplices that form the natural generalizations of the kagomé and pyrochlore lattices [18].

Since for  $SU(4)$  the difference of any two weights of the quark is a root and there are no others, the roots of  $SO(6)$  may just as well be written as

$$\Sigma(SO(6)) = \mu_i - \mu_j \quad [i \neq j : 1, 2, 3, \text{ or } 4] \quad (21)$$

a result we will invoke later.

The third minuscule representation of  $SO(6)$  is the 6-dimensional defining representation with weights

$$\mu = (\pm 1, 0, 0), \quad (0, \pm 1, 0), \quad (0, 0, \pm 1) \quad (22)$$

just as in  $Sp(6)$ . The decorated lattice again is made of corner-sharing octahedra, as shown in Fig. 4. However, without the long roots  $\pm 2\mathbf{e}_i$ , one can hop only along the edges but cannot jump directly from a point to its antipodal point.

This concludes the enumeration of lattices.

#### 2.3.4. Structure factor

Before we turn on the flux let us note that the structure factors for these lattices have a simple group theoretic interpretation. When we do a sum over all sites (indexed by  $l$ ) we find

$$\begin{aligned} S(\mathbf{k}) &= \sum_{l \in L_{2R} + \boldsymbol{\mu}} e^{i\mathbf{k} \cdot \mathbf{r}_l} = \sum_{L_{2R}} e^{i\mathbf{k} \cdot 2\mathbf{R}} \sum_{j \in \boldsymbol{\mu}} e^{i\mathbf{k} \cdot \boldsymbol{\mu}_j} = \sum_{L_{2R}} e^{i\mathbf{k} \cdot 2\mathbf{R}} \text{Tr} e^{i\mathbf{k} \cdot \mathbf{H}} \\ &\equiv S_{L_{2R}}(\mathbf{k}) \chi(\mathbf{k}) \end{aligned} \quad (23)$$

where  $\mathbf{H}_i = H_i$ , the  $i^{th}$  element of the Cartan subalgebra, whose  $j^{th}$  eigenvalue is  $\mu_j^i$ , and  $\chi(\mathbf{k}) = \text{Tr} e^{i\mathbf{k} \cdot \mathbf{H}}$  is just the character of the representation.

### 3. Flux Hamiltonians in $d = 2$ .

We will turn on fluxes by attaching arrows to each bond. The sense of the arrow will remain fixed as we move along bonds in any one direction. The hopping amplitude will be  $\pm i$  if we go along (against) the arrow. Time reversal reverses every arrow, sending  $H \rightarrow -H$ . Since time reversal also reverses  $\mathbf{k}$ , this means that in cases we study,

$$H(-\mathbf{k}) = -H(\mathbf{k}). \quad (24)$$

If all hopping amplitudes are pure imaginary, the flux through each triangle is  $\pm\pi/2$ . It is important to remember that the arrows themselves do not stand for physical quantities. For example a tetrahedron with uniform flux  $\pi/2$  coming out of each face is invariant under all symmetries of the tetrahedron although the arrows will look different if we say rotate the figure. This will, of course, be built into a PSG (Projective Symmetry Group) analysis [5].

#### 3.1. $SU(3)$ and kagomé

Let us begin with the first case, the kagomé lattice, now with the flux shown in Fig.7. Note that as we go counter-clockwise around the (quark) triangles 1-2-3-1, we get a product  $(i)(+i)(-i) = +i$ . This is so for every quark triangle. The antiquark triangles will have the opposite flux.

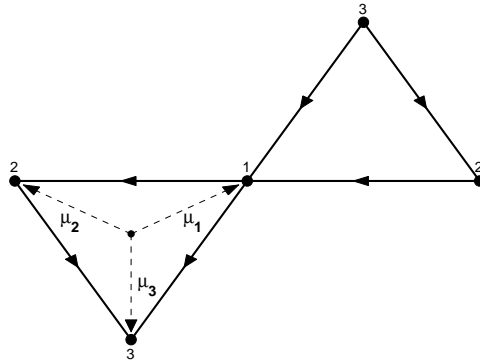


Fig. 7. Flux assignment on the kagomé lattice. There is a phase factor of  $\pm i$  as we move along (against) the arrow.

Consider hops from the site numbered 1 in the central unit cell shown, to the sites numbered 2 to its left (on the same cell) and right (on the cell to the right). Hopping along (against) the arrows brings a factor

of  $\pm i$ . We note that this state was one of several mean-field solutions found by [19] for uniform hopping on the kagomé lattice.

In terms of creation and destruction operators  $c$  and  $c^\dagger$  we have, in obvious notation, a contribution to  $H$  :

$$\begin{aligned} H_{1,2}(\mathbf{k}) &= c_2^\dagger c_1 \left( i e^{i\mathbf{k} \cdot (\boldsymbol{\mu}_2 - \boldsymbol{\mu}_1)} + h.c. \right) - (1 \leftrightarrow 2) \\ &= (c_2^\dagger c_1 + c_1^\dagger c_2) \sin(\mathbf{k} \cdot \boldsymbol{\alpha}_{12}) \end{aligned} \quad (25)$$

where we have dropped an overall factor of 2, suppressed the  $\mathbf{k}$  dependence of the operators, and as before,

$$\boldsymbol{\alpha}_{12} = \boldsymbol{\mu}_1 - \boldsymbol{\mu}_2 \quad (26)$$

Upon noting that  $c_1^\dagger c_2 = E_{\boldsymbol{\alpha}_{12}}$ , the generator corresponding to the root  $\boldsymbol{\alpha}_{12}$ , we see that when all hops are included we get what we shall the *canonical* form

$$H(\mathbf{k}) = \sum_{\Sigma^+} \sin(\mathbf{k} \cdot \boldsymbol{\alpha}) \left[ E_{\boldsymbol{\alpha}} + E_{\boldsymbol{\alpha}}^\dagger \right] \quad (27)$$

where the sum is over  $\Sigma^+$ , the positive roots, which have the form  $\mu_i - \mu_j$  with  $i < j$ .

In this paper we will often modify the canonical form in two ways: replace  $\sin(\mathbf{k} \cdot \boldsymbol{\alpha})$  by  $\mathbf{k} \cdot \boldsymbol{\alpha}$  and attach various signs  $s_{\boldsymbol{\alpha}} = \pm 1$  in front of each term so  $H$  assumes the more general form

$$H(\mathbf{k}, s_{\boldsymbol{\alpha}}) = \sum_{\Sigma^+} s_{\boldsymbol{\alpha}} \sin(\mathbf{k} \cdot \boldsymbol{\alpha}) (E_{\boldsymbol{\alpha}} + E_{\boldsymbol{\alpha}}^\dagger). \quad (28)$$

The role of these signs is to modify the relative phase of the hopping amplitudes on various bonds, and therefore the fluxes.

Putting in explicit values, we get for the canonical case

$$H(\mathbf{k}) = \begin{bmatrix} 0 & \sin x & \sin\left(\frac{1}{2}(x + \sqrt{3}y)\right) \\ \sin x & 0 & -\sin\left(\frac{1}{2}(x - \sqrt{3}y)\right) \\ \sin\left(\frac{1}{2}(x + \sqrt{3}y)\right) - \sin\left(\frac{1}{2}(x - \sqrt{3}y)\right) & 0 & 0 \end{bmatrix} \quad (29)$$

where  $x$  and  $y$  stand for  $k_x$  and  $k_y$  respectively.

The determinant of this matrix

$$|H| = -2 \sin x \sin\left(\frac{1}{2}(x - \sqrt{3}y)\right) \sin\left(\frac{1}{2}(x + \sqrt{3}y)\right) \quad (30)$$

shows zeros along the lines  $x = 0$  and  $x = \pm\sqrt{3}y$ , which are precisely the directions of the weights (or their negatives)! The determinant also has a simple form in terms of the three positive roots:

$$|H| = -2 \sin(\mathbf{k} \cdot \boldsymbol{\alpha}_{12}) \sin(\mathbf{k} \cdot \boldsymbol{\alpha}_{13}) \sin(\mathbf{k} \cdot \boldsymbol{\alpha}_{23}) \quad (31)$$

We do not know how this generalizes for  $SU(N)$ . But we do know how to understand the lines of zeros as follows.

The Hamiltonian has the form

$$\sum_{i < j} \sin(\mathbf{k} \cdot (\boldsymbol{\mu}_i - \boldsymbol{\mu}_j)) (E_{\boldsymbol{\alpha}_{ij}} + E_{\boldsymbol{\alpha}_{ij}}^\dagger) \quad (32)$$

Suppose we set  $\mathbf{k} = \boldsymbol{\mu}_1$ . (All points on the simplex are the same and we pick one that is easier to analyze.) The simplex has the property that

$$\boldsymbol{\mu}_i \cdot \boldsymbol{\mu}_j = \begin{cases} a & i = j \\ b & i \neq j \end{cases} \quad (33)$$

It follows that the argument of any sine in which  $\mu_1$  does not appear will vanish and the ones where it does will have the same value  $a - b$ . The resulting matrix, proportional to  $\sin(a - b)$ , has non-zero entries only in the first row or column. This leaves a  $2 \times 2$  submatrix of zeros which kills the determinant:

$$\sin(a - b) \left| \sum_{j=2}^3 (E_{\alpha_{1j}} + E_{\alpha_{1j}}^\dagger) \right| = 0 \quad (34)$$

This will happen for all  $SU(N)$  because each raising or lowering operator in the fundamental representation has only one non-zero entry. (Geometrically, this is equivalent to the statement that the  $N$ -simplex has no parallel edges). The components of the Hamiltonian which do not vanish for  $\mathbf{k} = \mu_1$  are

$$\sin(a - b) \sum_{j=2}^N (E_{1j} + E_{1j}^\dagger) \quad (35)$$

But all of these are hoppings to or from site 1, so that all non-zero entries lie in either the first row or the first column of the matrix. The resultant  $(N - 1) \times (N - 1)$  null submatrix ensures that the determinant is zero at this particular value of  $\mathbf{k}$ .

Let us now replace  $\sin x$  by  $x$ , since none of the key features are lost and the algebra is more manageable, especially in the problem of diagonalization. So we will set

$$H(\mathbf{k}) = \begin{pmatrix} 0 & x & \frac{1}{2}(x + \sqrt{3}y) \\ x & 0 & -\frac{1}{2}(x - \sqrt{3}y) \\ \frac{1}{2}(x + \sqrt{3}y) & -\frac{1}{2}(x - \sqrt{3}y) & 0 \end{pmatrix} \quad (36)$$

The determinant of this matrix is

$$|H| = -\frac{1}{2}x(x - \sqrt{3}y)(x + \sqrt{3}y) \quad (37)$$

which shows zeros along the same lines  $x = 0$  and  $x = \pm\sqrt{3}y$  as before.

If we change the sign of the term multiplying any of the generators, we get the same lines of zeros. This is expected since we simply reverse the flux penetrating every triangle, which inverts the spectrum. If we reverse the signs of any two of them, it makes no difference even to the flux. The reader can check the lines of zeros are not altered by any change of sign.

As explained earlier, this is a problem where  $H(\mathbf{k}) = -H(-\mathbf{k})$ , and the pair of points at  $\pm\mathbf{k}$  together produce  $E \rightarrow -E$  symmetry. With the Fermi energy at zero we are at half-filling, the relevant filling for mean-field solutions of the Heisenberg model.

The energies themselves are fairly complicated and not displayed here. It turns out two of them never vanish away from the origin and one of them produces all the zeros: if we move around the unit circle, it vanishes six times. Linearizing near these zeros will produce one-dimensional Dirac fermions that will control the low-energy physics. (Near the origin all six Dirac excitations will get mixed up.) If all this were part of a mean-field calculation, we would be looking at this Dirac field minimally coupled to a gauge field if we wanted to consider fluctuations. One could ask if the mean-field solution remains stable in their presence. These questions will be considered separately [20].

### 3.2. Flux Hamiltonians for $Sp(4)=SO(5)$

Recall that the groups  $Sp(4)$  and  $SO(5)$  are the same. The roots of one are the rotated and rescaled versions of the other and no new physics will come from looking at both. We will only work with  $SO(5)$  since it may be more familiar to the reader.

Before writing down the hopping matrix we need to define the basis. The states are numbered 1 through 4 in Fig. 8 with  $1 = (\frac{1}{2}, \frac{1}{2})$  etc. We use a tensor product of two Pauli matrices,  $\sigma$  and  $\tau$ , to operate on the two labels. We take as generators

$$\begin{aligned}
E_{\mathbf{e}_1} &= \frac{1}{2}\sigma_+ \otimes I = E_{-\mathbf{e}_1}^\dagger \\
E_{\mathbf{e}_2} &= \frac{1}{2}\sigma_3 \otimes \tau_+ = E_{-\mathbf{e}_2}^\dagger \\
E_{\mathbf{e}_1 \pm \mathbf{e}_2} &= \mp [E_{\mathbf{e}_1}, E_{\pm \mathbf{e}_2}] = \pm \frac{1}{2}\sigma_+ \otimes \tau_\pm \\
E_{-\mathbf{e}_1 \mp \mathbf{e}_2} &= E_{\mathbf{e}_1 \pm \mathbf{e}_2}^\dagger
\end{aligned} \tag{38}$$

### 3.2.1. The canonical Hamiltonian

In this basis we choose the canonical form

$$\begin{aligned}
H(\mathbf{k}) &= \sum_{\Sigma_+} (\mathbf{k} \cdot \boldsymbol{\alpha}) (E_{\boldsymbol{\alpha}} + E_{\boldsymbol{\alpha}}^\dagger) \\
&= \begin{pmatrix} 0 & y & x & x+y \\ y & 0 & y-x & x \\ x & y-x & 0 & -y \\ x+y & x & -y & 0 \end{pmatrix}.
\end{aligned} \tag{39}$$

The orientation of the arrows corresponding to this  $H$  are shown in Fig. 8. In other words, rather than write down some arrows and deduce the hopping matrix from these, we are writing down a canonical matrix in the Lie algebra and asking what hopping elements it implies.

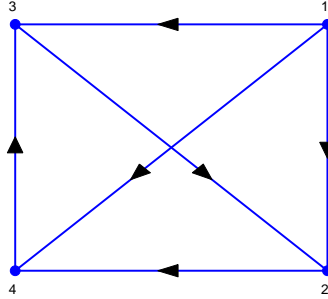


Fig. 8. Flux assignment for the canonical  $SO(5)$  Hamiltonian. There is a phase factor of  $\pm i$  as we move along (against) the arrow. The flux in each triangle alternates as we go counterclockwise in the case depicted.

If we look at the flux in each triangle we find that it alternates: triangles sharing a face diagonal, such as triangles 132 and 342 in Fig. 8, have the same flux, while triangles not sharing a face diagonal (triangles 132 and 142) have opposite flux. The determinant here is

$$|H| = 4(x^4 - x^2y^2 + y^4) \tag{40}$$

It has permutation symmetry but not full rotational symmetry. It has no zeros anywhere away from the origin. We do not know a simple way based on group theory to understand this.

The characteristic polynomial is

$$E^4 - 4E^2(x^2 + y^2) + 4(x^4 - x^2y^2 + y^4) \tag{41}$$

resulting in the particle-hole symmetric spectrum:

$$E = \pm \sqrt{2} \sqrt{x^2 + y^2 \pm \sqrt{3}xy} \tag{42}$$

The reason behind the symmetry  $E \rightarrow -E$  is the matrix

$$G = \begin{pmatrix} 0 & 0 & 0 & 1 \\ 0 & 0 & 1 & 0 \\ 0 & -1 & 0 & 0 \\ -1 & 0 & 0 & 0 \end{pmatrix}, \quad (43)$$

with  $G^2 = -I$ . Since

$$G \cdot H \cdot G^{-1} = -H \quad (44)$$

it follows that  $H$  and  $-H$  have the same spectrum.

The anatomy of the operator  $G$  is interesting. Suppose we wanted to manufacture an operator that reversed the sign of  $H$  by conjugation. We could accomplish this by a parity operation that exchanges each weight with its negative- this should flip every hopping term. However there are many ways to flip the weights since we can take each state to its parity reversed state, times any unimodular phase factor, which must be a sign if we want the hoppings amplitude to be  $\pm i$ . Suppose we picked a  $G'$  with all positive signs:

$$G' = \begin{pmatrix} 0 & 0 & 0 & 1 \\ 0 & 0 & 1 & 0 \\ 0 & 1 & 0 & 0 \\ 1 & 0 & 0 & 0 \end{pmatrix} \quad (45)$$

We would find

$$G' H G'^{-1} = \begin{pmatrix} 0 & -y & x & x+y \\ -y & 0 & y-x & x \\ x & y-x & 0 & y \\ x+y & x & y & 0 \end{pmatrix} \quad (46)$$

This is clearly not  $-H$ . However, if we go back to the lattice and ask what the corresponding hopping amplitudes are we will find that all the fluxes are reversed, though some arrows are reversed and some are not. Since  $-H$  also has all fluxes reversed (reversing every bond will reverse the product over every triangle) the two must be gauge equivalent. It turns out that appending minus signs to states 3 and 4 is one way to flip the arrows that needed to be flipped. The operator  $G$  is the product of  $G'$  and a diagonal matrix that multiplies 3 and 4 by minus signs. This is to be expected in a gauge theory, where the symmetry is projectively realized [5].

Since such a procedure will work for any self-conjugate representation, we will not explicitly construct the operator in future occasions.

We can understand now why the spectrum of  $H$  had the full set of lattice symmetries even though the flux alternated. Under any of the lattice symmetry operations, we either left the flux alone or reversed it. Neither affects the determinant since these operations at worst exchange  $E \rightarrow -E$ , which has no effect on the spectrum. This feature will be seen again when we consider other groups.

Since  $H$  is  $4 \times 4$ , and the characteristic equation is even in  $H$ , it satisfies an equation of the form

$$(H^2 - f(k) \cdot I)^2 = g(k) \cdot I \quad (47)$$

where  $f$  and  $g$  are scalar functions. Eq. (47) reduces to the Dirac form if  $g(k) = 0$  and  $f$  is constant.

### 3.2.2. The non-canonical Hamiltonian

Let us now change the sign in front of any of the terms in Eq. 39. It turns out that the determinant is sensitive only the relative sign of the two long roots that reach diagonally across the square. Here is what we get when we flip the coefficient of the  $E$  corresponding to the root  $\mathbf{e}_1 - \mathbf{e}_2$ :

$$H_{uni}(\mathbf{k}) = \begin{pmatrix} 0 & y & x & x+y \\ y & 0 & -(y-x) & x \\ x & -(y-x) & 0 & -y \\ x+y & x & -y & 0 \end{pmatrix} \quad (48)$$

If we compute the flux now, we find it is uniform in all triangles, hence the subscript in  $H_{uni}$ . This in turn means that  $H_{uni}$  will be invariant (up to gauge transformations) under symmetry operations of the lattice.

The characteristic polynomial is

$$E^4 - 4E^2x^2 - 4E^2y^2 + 4x^2y^2 \quad (49)$$

resulting in the spectrum

$$E = \pm\sqrt{2}\sqrt{x^2 + y^2 \pm \sqrt{x^4 + x^2y^2 + y^4}} \quad (50)$$

which has  $E \rightarrow -E$  symmetry because  $G$  once again anticommutes with  $H$ . The spectrum has zeros along the lines  $x = 0$  and  $y = 0$ . Note that along these directions,  $\alpha_{ij} \cdot \mathbf{e}_x = 1$  or  $0$ . As in the kagomé case, the lines of zeros are axes of symmetry of the unit cell. All edges not orthogonal to these axes have equal projections onto them (up to sign). With signs as in  $H_{uni}$ , this results in a pair of identical rows in the Hamiltonian – and thus lines of zeros along the short roots for both the linearized *and* lattice versions of  $H$ .

### 3.2.3. The Hamiltonian with unequal hopping

In the above we have considered a more general case

$$H(\mathbf{k}, s\alpha) = \sum_{\Sigma^+} s\alpha \sin(\mathbf{k} \cdot \alpha) (E\alpha + E\alpha^\dagger) \quad (51)$$

where  $s\alpha = \pm 1$  is a possible sign. In this problem there were essentially just two choices, the ones with uniform and alternating fluxes, determined by the relative sign of the two long hops.

In a problem like  $SO(5) = Sp(4)$ , where there are roots (i.e. bonds) of two different lengths, we could also play with the relative strengths of the hopping across long and short bonds. There is no obvious inspiration from group theory on how to choose from the continuum of possibilities, though only some choices will give  $SU(N)$  mean-field solutions. The only consolation is that only two different lengths are allowed for the roots of any semi-simple Lie algebra and among the cases we study this happens only for  $SO(2N+1)$  and  $Sp(2N)$ .

We just mention one extreme case where long hops are set equal to zero:

$$H_{short}(\mathbf{k}) = \begin{pmatrix} 0 & y & x & 0 \\ y & 0 & 0 & x \\ x & 0 & 0 & -y \\ 0 & x & -y & 0 \end{pmatrix} \quad (52)$$

Now the determinant is

$$|H_{short}| = (x^2 + y^2)^2 \quad (53)$$

which describes two Dirac points at the origin. Indeed, this is just the flux phase on the square lattice originally described by [3]. The unit cell is of course twice as big as it needs to be, so that the two Dirac points of the traditional unit cell have both come to the origin.

More generally, with a magnitude  $c$  for the long hops and relative signs all positive, the eigenvalues are

$$E = \pm\sqrt{(1+c^2)(x^2+y^2) \pm 2cxy\sqrt{c^2+2}} \quad (54)$$

and the spectrum has one Fermi point at the origin. For relative signs chosen as in  $H_{uni}$ , the eigenvalues are

$$E = \pm\sqrt{(1+c^2)(x^2+y^2) \pm 2c\sqrt{x^4+y^4+c^2x^2y^2}} \quad (55)$$



At the special values  $c = 0, \sqrt{2}$ , these give a Dirac spectrum. For all  $c \neq 1$ , the Fermi surface is a single point at the origin. Values of  $c$  corresponding to mean-field solutions are given in Section 5.1.

#### 4. Flux Hamiltonians in $d = 3$

Luckily we have to consider just three groups:  $SO(6)=SU(4)$ ,  $SP(6)$ , and  $SO(7)$ . The only minuscule representation of the latter is the spinor. There are three minuscule representations for  $SO(6)$ : two spinors (quark and antiquark of  $SU(4)$ ) and the six-dimensional vector representation.  $SP(6)$  has one minuscule representation– the defining one.

##### 4.1. Flux on the $SO(6)$ spinor lattice.

The weights forming the tetrahedron are

$$\boldsymbol{\mu}_1 = (\frac{1}{2}, \frac{1}{2}, \frac{1}{2}), \quad \boldsymbol{\mu}_2 = (-\frac{1}{2}, -\frac{1}{2}, \frac{1}{2}), \quad \boldsymbol{\mu}_3 = (\frac{1}{2}, -\frac{1}{2}, -\frac{1}{2}), \quad \boldsymbol{\mu}_4 = (-\frac{1}{2}, \frac{1}{2}, -\frac{1}{2}) \quad (56)$$

The positive roots are, in terms of orthogonal unit vectors,

$$\mathbf{e}_1 \pm \mathbf{e}_j \quad j > i = 1, 2, 3. \quad (57)$$

However, as pointed out in Eq. (21), it is more convenient to note that since this is also an  $SU(4)$  quark representation, we could write them in terms of the weights (56) as

$$\boldsymbol{\alpha}_{ij}^+ = \boldsymbol{\mu}_i - \boldsymbol{\mu}_j \quad j > i. \quad (58)$$

In view of what we saw in  $d = 2$  we are going to admit the more general case

$$H(\mathbf{k}, s\boldsymbol{\alpha}) = \sum_{\Sigma^+} s\boldsymbol{\alpha} \sin(\mathbf{k} \cdot \boldsymbol{\alpha})(E\boldsymbol{\alpha} + E\boldsymbol{\alpha}^\dagger) \quad (59)$$

where  $s\boldsymbol{\alpha} = \pm 1$  is a possible sign in front of each term.

##### 4.1.1. The canonical Hamiltonian

If we pick all signs positive, (which means the arrow always goes from a site with a lower index to one with a higher index) we obtain the flux assignment in Fig. 9(a). This gives the canonical Hamiltonian

$$H = \begin{pmatrix} 0 & x+y & y+z & x+z \\ x+y & 0 & z-x & z-y \\ y+z & z-x & 0 & x-y \\ x+z & z-y & x-y & 0 \end{pmatrix} \quad (60)$$

with determinant

$$|H| = 4x^4 - 4x^2y^2 - 4x^2z^2 + 4y^2z^2 \quad (61)$$

Note that it lacks the discrete symmetries of the lattice. This is to be expected since the flux on each face is not the same.

Consider its zeros. It vanishes along the weight directions,  $\mathbf{k} \propto \boldsymbol{\mu}_i$ . This is to be expected since the right-handed spinor is also the  $SU(4)$  quark representation and we have seen that for  $SU(N)$ , because the weights form a simplex, when  $\mathbf{k} \propto \boldsymbol{\mu}_i$  only terms corresponding to roots involving  $\boldsymbol{\mu}_i$  remain (and that all have the same coefficient in front). The rest vanish, so that  $H$  has just one nonzero row or column.

But we find in addition that there are entire planes along which there are zeros. For example for any linear combination  $\mathbf{k} = a\boldsymbol{\mu}_1 + b\boldsymbol{\mu}_2$  or  $\mathbf{k} = a\boldsymbol{\mu}_1 + b\boldsymbol{\mu}_4$ , the determinant vanishes. However it does not vanish for  $\mathbf{k} = a\boldsymbol{\mu}_1 + b\boldsymbol{\mu}_3$  unless  $a = 0$  or  $b = 0$ . This variation is to be expected since the flux is not symmetric on the tetrahedron.

Once again if we can use more powerful group theoretic methods to know when determinants of certain elements of the Lie algebra of the type of Eq. (59) will vanish, we will be able to anticipate this result rather than just observe it.

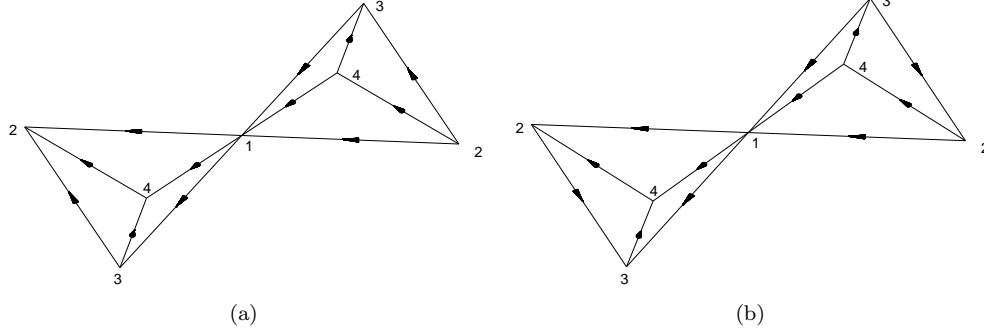


Fig. 9. Possible flux assignments to the pyrochlore. (a) Flux assignment breaking rotational symmetries. (b) Flux assignment preserving rotational symmetries.

#### 4.1.2. The uniform monopole case

If we flip the sign of the 24 and 42 matrix elements (corresponding to the root  $\mu_2 - \mu_4 = \alpha_{24}$ ) we obtain the flux assignment of Fig. 9(b). The Hamiltonian is

$$H_{mono} = \begin{pmatrix} 0 & x+y & y+z & x+z \\ x+y & 0 & z-x & -(z-y) \\ y+z & z-x & 0 & x-y \\ x+z & -(z-y) & x-y & 0 \end{pmatrix} \quad (62)$$

with determinant

$$|H_{mono}| = 4x^4 + 4y^4 + 4z^4 - 4x^2y^2 - 4x^2z^2 - 4y^2z^2 \quad (63)$$

which has the discrete symmetries of the lattice. The subscript on  $H_{mono}$  reflects the fact that the flux is the same on all faces of the tetrahedron and comes from a unit monopole at its center.

The reader may well ask how many more such signs are we going to play with. Luckily we are done.

To understand this, we need to transcribe the Hamiltonian to the corresponding factors of  $\pm i$  on the edges of the tetrahedron. As mentioned above, the case with all  $s\alpha = 1$  has a factor of  $i$  if we move from a corner to another with larger index (and a  $-i$  if we move the other way). It is readily verified that the two faces not involving the bond 24 have an outward flux of  $\frac{1}{2}\pi$  (a factor  $i$  around the triangular faces) and the other two the reverse. Clearly the choice of matrix elements violates the discrete symmetries of the tetrahedron.

On the other hand if we flip the coefficient of the  $\alpha_{24}$  term, we get an arrangement with all outward fluxes equal to  $\pi/2$  and we are led to  $H_{mono}$ , with a tetrahedrally symmetric determinant.

Other choices of sign will only yield one of two options: the flux is uniform (could be  $\pm\frac{1}{2}\pi$ ) and the determinant is symmetric, or the flux assignment breaks the symmetry with two positive and two negative faces. Different choices for the latter will correspond to determinants in which the asymmetric roles of  $x$ ,  $y$  and  $z$  are interchanged.

We will now elaborate further on the case  $H_{mono}$ , which describes uniform flux, as it has various nice properties. It has been discussed elsewhere as an interesting mean-field Hamiltonian for the  $SU(2)$  Heisenberg model on the pyrochlore lattice [21,22]. To make contact with existing literature on this problem, we will briefly revert to the custom of referring to momentum components as  $k_x$  or  $k_y$  rather than simply  $x$  or  $y$ .

The energy levels of  $H_{mono}$  are

$$E(k) = \pm \sqrt{2 \sum_i k_i^2 \pm 2 \sqrt{3 \sum_{(i < j)} k_i^2 k_j^2}} \quad (64)$$

The spectrum has  $E \rightarrow -E$  symmetry since there is a matrix  $G$  obeying  $G^2 = I$  that anticommutes with  $H_{mono}$ :

$$H_{mono}G = -GH_{mono} \quad (65)$$

where

$$G = \frac{1}{\sqrt{3}} \begin{bmatrix} 0 & 1 & 1 & 1 \\ -1 & 0 & 1 & -1 \\ -1 & -1 & 0 & 1 \\ -1 & 1 & -1 & 0 \end{bmatrix} \quad (66)$$

That a matrix  $G$  which ensures  $E \rightarrow -E$  symmetry should occur is less obvious than in the  $SO(5)$  case, since tetrahedron is not inversion symmetric (self-conjugate). The inversion operation maps the tetrahedron formed by the right-handed spinor representation of  $SO(6)$  to that formed by the left-handed representation. Hence  $G$  is not a simple geometric operation on sites in the unit cell.

We are tempted to cast  $H_{mono}$  in Dirac form

$$H_{mono} = \alpha_x k_x + \alpha_y k_y + \alpha_z k_z \quad (67)$$

since  $G$  seems to be like the matrix  $\beta$  which anticommutes with the three  $\alpha$ 's in the Dirac Hamiltonian. However the resemblance to the Dirac case is not complete because  $\alpha$ 's do not form a Clifford algebra and  $H_{mono}^2$  is not a multiple of the unit matrix.

What one finds is

$$\begin{aligned} [\alpha_i, \alpha_j]_+ &= 2\delta_{ij} + \sqrt{3}|\varepsilon_{ijk}|W_k \\ [W_i, W_j]_+ &= 2\delta_{ij}. \end{aligned} \quad (68)$$

In other words, the anticommutator of the  $\alpha$ 's is proportional to the unit matrix plus some amount of  $W$ 's, and the  $W$ 's obey a Pauli algebra. Thus if we square  $H(\alpha)$ , move the stuff proportional to the unit matrix to the left hand side and square again, we will end up with a multiple of the unit matrix. Indeed this is so:

$$(H^2 - 2k^2)^2 = 12(k_x^2 k_y^2 + k_x^2 k_z^2 + k_y^2 k_z^2) \quad (69)$$

where the subscript on  $H$  and the identity  $I$  have been suppressed.

That we should end up with the form encountered in the  $d = 2$   $SO(5)$  case of Eq. (47)

$$(H^2 - f(k) \cdot I)^2 = g(k)I \quad (70)$$

is due to the same reasons: the characteristic polynomial  $P(H)$  is even and of fourth order in  $H$ , i.e. quadratic in  $H^2$ . It can therefore be cast in the form Eq. (70). To get all details of  $f$  and  $g$  we would of course need to actually evaluate  $P(H)$ :

$$P(H) = H^4 - 4H^2(k_x^2 + k_y^2 + k_z^2) + 4(k_x^4 + k_y^4 + k_z^4 - k_x^2 k_y^2 - k_y^2 k_z^2 - k_z^2 k_x^2) = 0. \quad (71)$$

The anticommutator algebra in Eqs. (68) stems from the fact that the Hamiltonian lives in the Lie algebra of the right handed spinors of  $SO(6)$ , which is also the quark of  $SU(4)$ .

Recall that it is possible to write the generators of  $SO(N)$  in the spinor case in terms of the Dirac  $\gamma$ -matrices:  $\sigma_{\mu\nu}$ , which generates rotations in the  $\mu - \nu$  plane, may be expressed as  $\sigma_{\mu\nu} = \frac{i}{2}\gamma_\mu\gamma_\nu$ . Although the  $\gamma$  matrices are  $8 \times 8$ , bilinears in them like  $\sigma_{\mu\nu}$  form reducible representations with two  $4 \times 4$  blocks, these being the quark and antiquark of  $SU(4)$ . The two blocks are eigenstates of  $\gamma_7 = i\gamma_1 \cdots \gamma_6$  with eigenvalue  $\pm 1$ . If we want the quark we can work with these  $8 \times 8$  matrices and focus on just the top left hand corner. In this block  $\gamma_7$  is just a number equal to 1.

Consider the following operator

$$H = i\gamma_1(\gamma_6 - \gamma_4)k_x + i\gamma_3(\gamma_2 + \gamma_6)k_y + i\gamma_5(\gamma_4 + \gamma_2)k_z = H_R \oplus H_L \quad (72)$$

where  $H_R$  and  $H_L$  are  $4 \times 4$  blocks corresponding to right and left handed spinors, or quark and antiquark representations.

With a judicious choice of basis for the  $\gamma$  matrices its upper left-hand corner,  $H_R$  is just our Hamiltonian  $\alpha_x k_x + \alpha_y k_y + \alpha_z k_z$ . Thus if we do not stray from this block we can view the  $\alpha$ 's as bilinears of  $\gamma$  matrices. Not so obvious is the fact that the  $W$ 's which come from two powers of  $\alpha$  are also bilinears in  $\gamma$ .

The closure under anticommutation of the  $\sigma_{\mu\nu}$  or the  $\alpha$ 's and  $W$ 's is a special property of  $SO(6)$ . In general, if you multiply two of them you will get something quartic in the  $\gamma$ 's even after some of them reduce to quadratic terms upon invoking  $\gamma^2 = I$ . The quartic ones can be rewritten as  $\gamma_7$  times a quadratic, upon inserting the square of the “missing” two  $\gamma$  matrices. In the sector with  $\gamma_7 = 1$ , these are just quadratic in the  $\gamma$ 's.

#### 4.2. Flux on the $SO(6)$ vector lattice.

In the defining vector representation the generators are represented as follows in terms of canonical creation and destruction operators  $c$  and  $c^\dagger$ :

$$\begin{aligned} H_i &= c_i^\dagger c_i - c_{-i}^\dagger c_{-i} \quad i = 1, 2, 3 \\ E_{\mathbf{e}_i \mp \mathbf{e}_j} &= c_i^\dagger c_{\pm j} - c_{\mp j}^\dagger c_{-i} \quad i < j \leq 3 \end{aligned} \quad (73)$$

with generators of negative roots defined as the adjoints of the positive ones above.

##### 4.2.1. The canonical Hamiltonian

In this basis the usual sum over positive roots with all coefficients positive yields the matrix

$$H = \begin{pmatrix} 0 & 0 & x-y & x+y & x-z & x+z \\ 0 & 0 & -x-y & y-x & -x-z & z-x \\ x-y & -x-y & 0 & 0 & y-z & y+z \\ x+y & y-x & 0 & 0 & -y-z & z-y \\ x-z & -x-z & y-z & -y-z & 0 & 0 \\ x+z & z-x & y+z & z-y & 0 & 0 \end{pmatrix} \quad (74)$$

where the rows and columns are numbered as follows:  $(1, 0, 0) \equiv 1$ ,  $(-1, 0, 0) \equiv -1$ ,  $(0, 1, 0) \equiv 2$ ,  $\dots (0, 0, -1) \equiv -3$ , the components being just the eigenvalues of  $H_1$ ,  $H_2$  and  $H_3$ . The site labels and corresponding factors of  $\pm i$  are shown in Fig. 10. Note that the flux alternates from one face to the next.

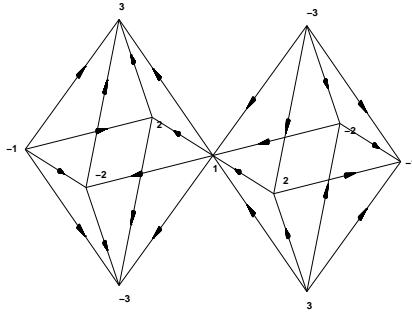


Fig. 10. Flux assignment to the octachlore in accordance with signs of the group generators of the vector representation of  $SO(6)$ .

The determinant vanishes identically because there are two zeros at every  $\mathbf{k}$ . If we pull them out we find

$$|H| = 48(x^2y^2 + y^2z^2 + z^2x^2) * 0 * 0 \quad (75)$$

that is to say, the product of the nonzero energies is  $48(x^2y^2 + y^2z^2 + z^2x^2)$ .

Why does  $H$  have all the discrete symmetries when the flux alternates? The answer is that any rotation is equivalent to a change of the sign of the overall flux, which in turn corresponds to time-reversal, and does not affect the determinant in a problem with  $E \rightarrow -E$  symmetry.

Extra zero-energy bands occur when any two coordinates vanish, i.e., along the axes, which corresponds to the direction of the weights. We can understand this to the extent we could understand the  $SU(N)$  and  $SO(5)$  cases. If

$$H = \sum_{i < j} (\mathbf{k} \cdot (\mathbf{e}_i \pm \mathbf{e}_j)) \left[ E_{\mathbf{e}_i \pm \mathbf{e}_j} + E_{\mathbf{e}_i \pm \mathbf{e}_j}^\dagger \right] \quad (76)$$

it follows that if we set  $\mathbf{k} = \mathbf{e}_1$  say, only roots of the form  $\mathbf{e}_1 \pm \mathbf{e}_j$  will survive and that too with the same coefficient. The matrix will have only two non-zero rows and columns – for the sites at  $\pm \mathbf{e}_1$  in the unit cell. With the flux assignment of (74), one row is exactly the negative of the other, resulting in two extra zero energy bands in both the linearized and the lattice Hamiltonian.

Near any line of zeros we can define a 2 dimensional Dirac field, except near the origin when they all collide and modify each other.

Again there is a matrix  $G$  which anticommutes with the Hamiltonian, and acts upon the unit cell as the inversion. Its existence results from the fact that the unit cell is inversion symmetric, while the directions of all fluxes are reversed by inversion.

#### 4.2.2. The non-canonical Hamiltonians

We could append signs for each term, but this gives spectra which break the lattice symmetries. We have not looked deeply into what kind of zeros result in that case.

We did however note the following. Suppose we start with a hopping problem on an octahedron with uniform flux in every face as in Fig. 11.

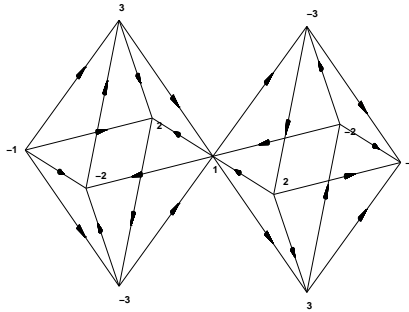


Fig. 11. Flux assignment to the octachlore preserving rotational symmetries.

When we extracted the  $H(\mathbf{k})$  for that problem we found it could not be written in terms of generators of  $SO(6)$ . It is important to understand why we have this problem here but did not when we considered the spinor of  $SO(6) =$  quark of  $SU(4)$ . There each root or generator connected only two states. If we did not like the sign of the matrix element given by group theory we just put a negative sign in front of that generator using  $s_{\alpha}$ . But here, each root connects two pairs of points, corresponding to parallel edges of the octahedron. For example

$$E_{\mathbf{e}_1 + \mathbf{e}_2} = c_1^\dagger c_{-2} - c_2^\dagger c_{-1} \quad (77)$$

connects points labeled  $(-2, 1)$  and  $(-1, 2)$  in Fig. 11 with *opposite* matrix elements. If we do not like the relative sign, we cannot do anything about it. This is exactly what happens in the case of the octahedron with uniform flux in every face. To describe it, we would have to use the generators of the much larger group

SU(6). But that is not the game we are playing: we want to work within a group,  $SO(6)$  being the operative one here.

This could have happened to the  $SO(5)$  spinor, whose short roots connected opposite sides of the square with same sign for the horizontal roots  $\pm \mathbf{e}_1$  and opposite signs for the vertical roots  $\pm \mathbf{e}_2$ . Luckily this choice of signs corresponded to the case of interest.

#### 4.3. $Sp(6)$

The defining representation of  $Sp(6)$  is the same octahedron as in  $SO(6)$  with the same weights. The generators can be written in terms of creation and destruction operators as

$$\begin{aligned} H_i &= c_i^\dagger c_i - c_{-i}^\dagger c_{-i} \quad i = 1, 2, 3 \\ E_{\mathbf{e}_i \mp \mathbf{e}_j} &= c_i^\dagger c_{\pm j} \mp c_{\mp j}^\dagger c_{-i} \quad i < j \leq 3 \\ E_{2\mathbf{e}_i} &= 2c_i^\dagger c_{-i} \end{aligned} \tag{78}$$

with negative roots being given by adjoints of the above.

##### 4.3.1. *The non-canonical Hamiltonian*

It is interesting to consider first the canonical  $H$  with all signs positive and *only the short roots*. (As noted before when we have two different root lengths, we have the freedom to chose the scale of each type of term. Keeping only short roots is an extreme case.) We find

$$H_{short}(\mathbf{k}) = \begin{pmatrix} 0 & 0 & x-y & x+y & x-z & x+z \\ 0 & 0 & x+y & y-x & x+z & z-x \\ x-y & x+y & 0 & 0 & y-z & y+z \\ x+y & y-x & 0 & 0 & y+z & z-y \\ x-z & x+z & y-z & y+z & 0 & 0 \\ x+z & z-x & y+z & z-y & 0 & 0 \end{pmatrix} \tag{79}$$

The determinant has the value

$$|H_{short}| = -32(x^2 + y^2)(x^2 + z^2)(y^2 + z^2) \tag{80}$$

that is to say, zeros along the weights. The logic is the same as in  $SO(6)$  since the long roots that distinguish between them have been suppressed. Note however that matrix elements are different now: the two pairs of states connected by a generator do not always have opposite matrix elements. Thus in this case along the axes there are 2, rather than 4, zero energy bands.

What is surprising is that the energies do not change *for any choice of signs* !

##### 4.3.2. *A non-canonical Hamiltonian with unequal coefficients*

Consider the following matrix involving the long roots:

$$H_{\text{"}x+z\text{"}, \frac{1}{2}} = \begin{pmatrix} 0 & 2x & x-y & x+y & x-z & -x-z \\ 2x & 0 & x+y & y-x & -x-z & z-x \\ x-y & x+y & 0 & 2y & y-z & y+z \\ x+y & y-x & 2y & 0 & y+z & z-y \\ x-z & -x-z & y-z & y+z & 0 & 2z \\ -x-z & z-x & y+z & z-y & 2z & 0 \end{pmatrix} \quad (81)$$

where the subscripts remind us of two ways in which it differs from the canonical form: the  $x+z$  term has a minus sign relative to the canonical form, and the hopping matrix element for the long roots is half as big as the canonical one. As for the latter point, consider the term  $2x$ . It indeed equals  $\mathbf{k} \cdot 2\mathbf{e}_1$ , but the generator  $E_{2\mathbf{e}_1} = 2c_1^\dagger c_{-1}$  has another two in it. So this term should have been  $4x$ . But with the choice of sign and hopping (81) we get

$$|H_{\text{"}x+z\text{"}, \frac{1}{2}}| = -16(x+y)^2(x+z)^2(y+z)^2 \quad (82)$$

which has zeros along planes  $x+y=0$  etc.

When we put in the canonical strength ( $4x$  etc.) we did not find any interesting spectra for many choices of sign that we tried.

#### 4.4. $SO(7)$ spinor

Recall that the only minuscule representation of  $SO(7)$  is the spinor and that the lattice we associate with it is cubic, with face diagonals but no body diagonals (Fig. 12(a)). The generators in this representation can be expressed in the direct product space of three Pauli matrices:

$$\begin{aligned} E_{\pm\mathbf{e}_1} &= \frac{1}{2}\sigma_3 \otimes \tau_3 \otimes \alpha_{\pm} & E_{\pm\mathbf{e}_2} &= \frac{1}{2}\sigma_3 \otimes \tau_{\pm} \otimes 1 \\ E_{\pm\mathbf{e}_3} &= \frac{1}{2}\sigma_{\pm} \otimes 1 \otimes 1 & E_{\mathbf{e}_1 \pm \mathbf{e}_2} &= \pm \frac{1}{2}1 \otimes \tau_{\pm} \otimes \alpha_{\pm} \\ E_{\mathbf{e}_1 \pm \mathbf{e}_3} &= \pm \frac{1}{2}\sigma_{\pm} \otimes \tau_3 \otimes \alpha_{\pm} & E_{\mathbf{e}_2 \pm \mathbf{e}_3} &= \pm \frac{1}{2}\sigma_{\pm} \otimes \tau_{\pm} \otimes 1 \end{aligned} \quad (83)$$

where the labels 1, 2, and 3 correspond to the directions of the co-ordinate axes.

The matrix

$$G = \sigma_2 \otimes \tau_1 \otimes \alpha_2 \quad (84)$$

acts as an inversion operator on the unit cell and anti-commutes with *all* of the symmetric generators  $E_{\alpha} + E_{-\alpha}$  so that the spectrum has symmetry under  $E \rightarrow -E$  no matter what the signs.

##### 4.4.1. The canonical Hamiltonian

If we ask what hopping amplitudes are associated with the canonical case we find that each square plaquette has  $\pi$  flux.

The generators  $E_{i \pm j}$  fix the flux through the triangular plaquettes to be  $\pm\pi/2$ . The form of these generators dictates that two opposing pairs of triangular faces will have diagonals with the same orientation; the third will have diagonals with opposite orientations. It turns out that in this case a uniform flux through the triangular plaquettes is impossible.

If we choose all signs to be positive, then three of the cube's faces have flux  $\pi/2$  outwards through all triangular plaquettes, and the remaining three to have flux  $-\pi/2$ .

The zeros of energy can be found from

$$|H| = \frac{1}{256}(x^2 + y^2 + z^2 - 2(xz - yz - xy))^2(x - y + z)^4 \quad (85)$$

Here not all cubic symmetries are preserved, but permutations of the  $x$ ,  $-y$ , and  $z$  axes (corresponding to rotations of the cube about the  $(1, -1, 1)$  body diagonal) map positive fluxes to positive fluxes and vice versa, so that some of the cubic symmetries are preserved.

#### 4.4.2. The non-canonical Hamiltonian with alternating flux

As in the octahedral case, the other interesting case is the alternating flux pattern shown in Fig. 12(b), in which rotations by  $\pi/4$  about the  $x$ ,  $y$ , and  $z$  axes reverse the signs of all fluxes. In this case, we append minus signs to the  $x + z$ ,  $x - y$ , and  $y - z$  terms. The energies are remarkably simple:

$$E = \pm \frac{1}{2} \sqrt{3} (x \pm y \pm z) \quad (86)$$

which vanish along the planes  $x = \pm y \pm z$ . For example, if the sites of the unit cell are labeled 1 – 8 as shown in Fig. 12(b), momenta in the plane  $x = -y - z$  obey  $\mathbf{k} \cdot \boldsymbol{\alpha}_{1j} = -\mathbf{k} \cdot \boldsymbol{\alpha}_{8j}$ , producing a pair of linearly dependent rows in the Hamiltonian. In the alternating flux case the cubic symmetries are preserved since a  $\pi/4$  rotation reverses the signs of all fluxes, which is gauge equivalent to reversing the signs of all hoppings and thus the sign of  $H$ . Invariance under  $E \rightarrow -E$  thus ensures that this is a symmetry.

These two possibilities are the only ones preserving the permutation symmetry of the  $x$ ,  $y$  and  $z$  axes.

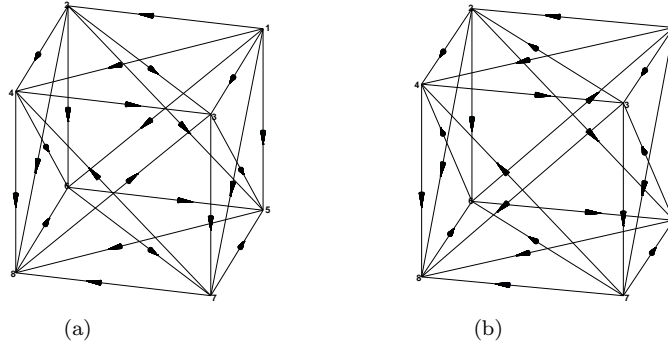


Fig. 12. Two possible flux assignments for on the  $SO(7)$  lattice. Each square plaquette has flux  $\pi$ , while the triangular plaquettes on each face may be chosen to have equal (a) or alternating (b) flux.

## 5. Comments

### 5.1. Relevance to mean-field solutions of the Heisenberg model

We will now revisit the Hamiltonians of Sections 3 and 4 with a view to asking whether they are, in fact, mean-field solutions of the  $SU(N)$  Heisenberg model. A few of these have been discussed previously in the literature. The kagomé Hamiltonian of Section 3.1 was identified as a mean-field solution by [19]. Several authors have discussed  $SU(N)$  mean-field states on the square lattice with second neighbour hopping [9,8,23,24], though these have focused on the gapped chiral spin state quite unlike that of Section 3.2; we believe that previous mean-field studies on the checkerboard lattice [25] have been restricted to dimerized states.

We wish to extend these results and establish that many of the Hamiltonians discussed above are mean-field solutions. To show this, we must argue that the mean-field equations admit solutions in which the hoppings  $t_\alpha$  are purely imaginary, and hoppings along roots of equal length are equal in magnitude.

The mean-field equation can be written [8]

$$t_{ij} = \frac{J_{ij}}{\pi^2} \int_{q \in 1BZ} \sum_{E^{(n)}(\mathbf{k}) < 0} \frac{1}{|E^{(n)}(\mathbf{k})|} H_{ij}(\mathbf{k}) e^{-i\mathbf{k} \cdot \mathbf{r}_{ij}} \quad (87)$$

where  $J_{ij}$  is the spin-spin coupling between sites  $i$  and  $j$  for the original Heisenberg Hamiltonian, and  $t_{ij}$  is the hopping matrix element between these sites for the mean-field Hamiltonian. If the spectrum is invariant under  $k \rightarrow -k$ , then  $H(k) = -H(-k)$  guarantees that the real part of the integral vanishes. Further, if



the spectrum preserves the lattice symmetries, then the integral will clearly have the same magnitude for all roots  $\alpha_{ij}$  of a given length. In cases with two different length roots, the mean-field equations specify a particular relative hopping strength.

The reader should be warned, however, that some of the Hamiltonians we have studied have large manifolds of zero energy, such as planes of zeros. These may lead to a divergent integral in (87), in which case the Hamiltonian is *not* a mean-field solution.

Such exceptions aside, many of the flux configurations discussed in Sections 3 and 4 do clearly give self-consistent mean-field Hamiltonians. Consider first the lattices in which all links have the same length (and are related by lattice symmetries): the kagomé, pyrochlore, and octachlore. In these cases (87) gives equal hopping amplitudes on all links provided that the spectrum does not break the lattice symmetries. The kagomé Hamiltonian has been discussed by [19]; it is somewhat exceptional among the Hamiltonians we consider in that its spectrum is not inversion symmetric at fixed  $\mathbf{k}$ . The monopole Hamiltonian of the pyrochlore lattice (Section 4.1.2), as well as  $SO(6)$  (Section 4.2.1) and short-root  $SP(6)$  (Section 4.3.1) Hamiltonians on the octachlore lattice have spectra that preserve lattice symmetries and thus naively should be mean-field states by the argument above. We have verified numerically that the monopole and short-root  $SP(6)$  Hamiltonians are viable mean-field solutions. The  $SO(6)$  Hamiltonian on the octachlore lattice, however, has two bands of zero energy, causing (87) to diverge; it is not a mean-field solution.

The lattices constructed from the spinor representation of  $SO(2N+1)$ , as well as the canonical lattice of  $SP(2N)$ , have roots of two different lengths. In all three examples discussed here, Hamiltonians with hopping only along the short roots are mean-field solutions; for  $SO(5)$  this gives the flux state of [3] and for  $SO(7)$  the 3-d version thereof. If we are interested in Hamiltonians with non-zero hopping along the long roots, we must find the ratio  $t_l/t_s$  consistent with Eq. (87).

A summary of the allowed values of  $t_l/t_s$  is given in Table 5.1. For  $SP(6)$  generic values of  $t_l/t_s$  do not give symmetric spectra, and we find no mean-field Hamiltonians with  $t_l > 0$ . The alternating flux Hamiltonian of  $SO(7)$  has a symmetric spectrum for general  $t_l/t_s$ ; however for many  $t_l/t_s$  two-dimensional surfaces of zero energy cause the integral to diverge and we are unable to find a mean-field solution with  $t_l > 0$ . Both flux assignments discussed in Section 3.2 for the  $SO(5)$  spinor lattice give symmetry-preserving spectra whose mean-field  $t_l/t_s$  can be calculated numerically. The ratio  $t_l/t_s$  at mean-field depends on the relative magnitudes of the spin-spin coupling  $J_l/J_s$  in the original Heisenberg Hamiltonian; solutions with  $t_l > 0$  exist only for sufficiently large  $J_l$ , as shown in Table 5.1.

	$SO(5)$ (alt)	$SO(5)$ (uni)	$SO(7)$ (alt)	$SP(6)$
$J_l/J_s$	$t_l/t_s$	$t_l/t_s$	$t_l/t_s$	$t_l/t_s$
1	0, 1.59	0, 2.28	0	0
.9	.371	1.66	0	0
.8	0	1.28	0	0
.7	0	1.07	0	0

Table 1

Relative strengths of hopping along the long ( $t_l$ ) and short ( $t_s$ ) roots as determined by the mean-field equations for the  $SO(5)$ ,  $SO(7)$ , and  $SP(6)$  hopping problems. For  $SP(6)$  and  $SO(7)$  we find only the  $t_l = 0$  solution at mean-field level. For  $SO(5)$  we find consistent mean-field solutions with  $t_l > 0$  for  $J_l/J_s > .682$  in the uniform flux case, and .891 in the alternating flux case.

Needless to say, this analysis does not preclude the existence of other flux assignments leading to a lower mean-field energy. Indeed states with lines and planes of zeros, as many of our examples have, are often energetically disfavoured at mean-field [19] due to the large phase space near  $E = 0$  relative to gapped or mostly gapped states. Also one must bear in mind that dimerized mean-field states of lower energy inevitably exist [11,12]. However, as pointed out in Section 1.1, corrections to the mean-field solution for  $N < \infty$  often alter the relative stability of various mean-field states, so we should not take this issue too seriously. Among the mean-field solutions discussed here, an interesting example of this is the monopole Hamiltonian of the pyrochlore lattice. It corresponds to the lowest energy symmetry preserving mean-field solution to the  $SU(N)$  Heisenberg model, and has lower energy than the dimerized mean-field ground states after Gutzwiller projection is used to enforce the constraint of single occupancy [22].

### 5.2. Hamiltonians beyond the linear approximation

This work has focused on the linearized versions of lattice Hamiltonians, in which we have replaced

$$\sin(\mathbf{k} \cdot \mathbf{r}) \rightarrow \mathbf{k} \cdot \mathbf{r}. \quad (88)$$

However, many of the interesting properties of the spectra are unaffected by this substitution.

First, surfaces of zero energy which are related to symmetries of the unit cell will not be affected. Recall that we find several zero-energy surfaces along directions of the unit cell for which  $\mathbf{k} \cdot \mathbf{r}_{ij}$  takes on values  $\pm c, 0$  for some constant  $c$ . If  $\mathbf{k} \cdot \mathbf{r}_{ij}$  is replaced by  $\sin(\mathbf{k} \cdot \mathbf{r}_{ij})$ , the only effect on the Hamiltonian at these points is to change the value of the constant  $c$ ; hence the zero eigenvalues remain. As discussed above, this yields lines of nodes along the weight vectors for the  $SU(N)$  lattice model for any  $N$ . The zero-energy manifolds of the alternating flux  $SO(5)$  and  $SO(7)$  Hamiltonians, and the  $SO(6)$  and  $SP(6)$  Hamiltonians discussed above for the octachlore lattice, are also preserved under (88). In other words, all zero-energy surfaces listed in Sections 3 and 4 which reflect symmetries of the lattice unit cell are unaffected by the substitution (88).

Second, the symmetry of the spectrum will remain. Symmetries in the spectra occur when flux is assigned in a way that preserves the lattice symmetries, and the substitution (88) cannot alter the symmetry properties of the state.

Finally, it is interesting to note that on the lattices with inversion-symmetric unit cells (namely lattices related to representations of  $SO(N)$  or  $SP(2N)$ ), the operator  $G$  which anti-commutes with the linearized Hamiltonian also anti-commutes with the lattice Hamiltonian. This happens because  $G$  in these cases is simply the inversion operator multiplied by an appropriate gauge transformation, and inversion maps every edge to another edge associated with the same symmetric generator of the Lie group representation. Thus  $G$  anti-commutes separately with all of the symmetric generators – and hence also with the lattice Hamiltonian  $\sum_{\Sigma+} (E_{\alpha} + E_{\alpha}^{\dagger}) \sin(\mathbf{k} \cdot \mathbf{r}_{\alpha})$ .

### 5.3. Extensions to Higher Dimensions

We have already noted that the generalization of our Hamiltonians to  $d \geq 4$  is problematic. For completeness we note here that the lattice construction described in Section 2 can be applied to the appropriate representations of the Lie groups discussed above in arbitrary dimension. Assigning a hopping of  $\pm i$  to each directed edge will result in a Hamiltonian related to the group generators by Eq. (28), for which  $H(\mathbf{k}) = -H(-\mathbf{k})$ . Additionally, for all of the cubic lattices ( $SO(N)$  spinor,  $SO(2N)$  vector, and the defining representation of  $Sp(2N)$ ) a matrix  $G$  can be found which anti-commutes with the Hamiltonian, leading to a time-reversal invariant spectrum.

In general, however, the symmetry operations of the resulting unit cell make it impossible to assign flux in such a way that the lattice symmetries are unbroken. The notable exception is the  $SO(2N+1)$  spinor case with only the short roots, where all fluxes are  $\pi \equiv -\pi$ . This gives the  $N$  dimensional Dirac Hamiltonian.

## 6. Conclusions and Outlook

In this paper we constructed a class of lattices inspired by the root and weight systems of Lie algebras. The lattices had as their unit cells minuscule representations of the standard Lie groups which decorated the underlying lattice  $L_{2R}$ , elements of the root lattice with even coefficients. We observed that the lattices could equally well be viewed as decorations of  $L_{2R}$  by the conjugate representation, which shared corners with the original one. While construction works for any rank  $r$  we stuck to  $r = 2, 3$  since these were experimentally accessible and because these allowed an unambiguous assignment of flux on the triangular faces of the unit cells. Remarkably, they also correspond in many cases to known lattices like the pyrochlore, kagomé or checkerboard. Even our octachlore lattice is a motif in the perovskite structure.

We find this last aspect enticing, for it hints that it may be possible to relate more physics on these lattices to the underlying Lie algebras. Indeed, as we were finishing up this work we came across recent work by Arovas [26] who constructs generalized AKLT models on the kagomé and pyrochlore lattices which

naturally involve local degrees of freedom that live in the fundamental representations of  $SU(3)$  and  $SU(4)$  respectively.

However, our own work makes a different connection. We considered hopping Hamiltonians which, when written in momentum space, were elements of the Lie algebra, linear in the momentum  $\mathbf{k}$  for small  $\mathbf{k}$ , and obeyed  $H(\mathbf{k}) = -H(-\mathbf{k})$ .<sup>3</sup> By varying the signs in front of each generator we could alter the fluxes in the faces of the unit cell. We found Dirac or Dirac-like spectra at points, lines and even sheets. The locus of the zeros had strong ties to the directions of the weights or roots. We could anticipate and thus understand some of them using ideas from Lie algebras but often were just able to draw attention to them. It seems very likely that an assault using ideas from Lie algebras can yield further understanding. To begin with one must employ a more systematic way to represent weights and roots in dual bases: simple weights for the former and simple roots for the latter. One should also use color groups to classify symmetries of this problem where the triangular faces of the unit cell are colored with flux  $\pm\pi/2$ . Of all the properties associated with  $H$ , the determinant seems most likely to yield to group theoretic methods. It has uniformly proven to be a much simpler and more symmetric function of the momenta than individual eigenvalues.

The spectra often had  $E \rightarrow -E$  symmetry. For self-conjugate representations we could fully understand this feature and indeed use our understanding to construct an operator  $G$  that anticommuted with the Hamiltonian and explained this feature.

While such hopping problems typically arise as lattice regulators for continuum theories or as mean-field theories for quantum spin models, in this paper we have studied them in their own right. While we did observe that most of them are candidates for interesting mean-field theories of quantum Heisenberg models on the same lattices, a fuller investigation of the fluctuations would be required to establish their value in that setting.

We hope that some readers will be sufficiently intrigued by the connections that we have sought to establish in this paper to go on and grapple with them on their own.

## 7. Acknowledgements

R. Shankar thanks Professors Greg Moore and Siddhartha Sahi from Rutgers and Professor Greg Zuckerman from Yale for helpful discussions, the National Science Foundation for grant DMR-0354517, and the Princeton Center for Theoretical Physics for its hospitality during the course of this work. F. Burnell and S. L. Sondhi thank Shoibal Chakravarty for a prior collaboration which inspired this project. F. Burnell acknowledges the support of NSERC. S. L. Sondhi would like to acknowledge support from NSF Grant No. DMR 0213706.

## References

- [1] G. Baskaran, P. W. Anderson, Phys. Rev. B 37 (1) (1988) 580–583.
- [2] G. Baskaran, Z. Zou, P. W. Anderson, Solid State Commun. 63 (11) (1987) 973–976.
- [3] J. B. Marston, I. Affleck, Phys. Rev. B 39 (1989) 11538.
- [4] M. Hermele, T. Senthil, M. P. A. Fisher, P. A. Lee, N. Nagaosa, X.-G. Wen, Phys. Rev. B 70 (2004) 214437.
- [5] X.-G. Wen, Phys. Rev. B 65 (2002) 165113.
- [6] M. B. Hasgins, Phys. Rev. B 63 (2000) 014413.
- [7] Y. Ran, M. Hermele, P. A. Lee, X.-G. Wen, Phys. Rev. Lett. 98 (2007) 117205.
- [8] R. B. Laughlin, Z. Zou, Phys. Rev. B 41 (1989) 664.
- [9] X.-G. Wen, F. Wilczek, A. Zee, Phys. Rev. B 39 (1989) 11413.
- [10] V. Kalmeyer, R. B. Laughlin, Phys. Rev. Lett. 59 (18) (1987) 2095–2098.
- [11] D. S. Rokhsar, Phys. Rev. B 42 (1990) 2526.
- [12] N. Read, S. Sachdev, Phys. Rev. B 42 (7) (1990) 4568–4589.
- [13] H. Georgi, Lie Algebras in Particle Physics, 2nd Edition, HarperCollins, 1999.

---

<sup>3</sup> To belabor this point, we have an entire unit cell represented by a quark state, while Arovas has a quark state at each site of the unit cell.

- [14] J.-Q. Chen, J. Ping, F. Wang, Group Representation Theory for Physicists, 2nd Edition, World Scientific Publishing Co., 2002.
- [15] M. Hamermesh, Group Theory and its applications, Addison Wesley, New York, 1962.
- [16] R. Lifshitz, Rev. Mod. Phys 69 (1997) 1181, 1218.
- [17] J. Kogut, L. L. Susskind, Phys. Rev. D 11 (2) (1975) 395–408.
- [18] S. Torquato, F. Stillinger, J. Appl. Phys 102 (2007) 093511.
- [19] J. B. Marston, C. Zeng, J. Appl. Phys. 69 (1991) 5962.
- [20] F. J. Burnell, S. L. Sondhi, in progress.
- [21] S. Chakravarty, PhD thesis, Princeton University (2004).
- [22] F. J. Burnell, S. Chakravarty, S. L. Sondhi, to appear.
- [23] M. Hermele, T. Senthil, M. P. A. Fisher, Phys. Rev. B 72 (2005) 104404.
- [24] R. B. Laughlin, Z. Zou, Phys. Rev. B 42 (1990) 4073.
- [25] J.-S. Bernier, C.-H. Chung, Y. B. Kim, S. Sachdev, Phys. Rev. B 69 (21) (2004) 214427.
- [26] D. Arovas, cond-mat.str-el/0711.3921.